Applied Catalysis B: Environmental 327 (2023) 122433

Contents lists available at ScienceDirect

Applied Catalysis B: Environmental

journal homepage: www.elsevier.com/locate/apcatb

Direct ethyl acetate synthesis from ethanol over amorphous-, monoclinic-, tetragonal ZrO_2 supported copper catalysts prepared from the same zirconium source

Takashi Yamamoto *, Hirotaka Mine, Shoki Katada, Taketo Tone

Department of Science and Technology, Tokushima University, Tokushima 770-8506, Japan

ARTICLE INFO

Keywords:
Direct ethyl acetate synthesis
Copper
ZrO_2
Crystalline phase
Amorphous

ABSTRACT

Direct ethyl acetate synthesis from ethanol was examined by supported Cu catalysts on various kinds of acid-base metal oxides, available ZrO_2-based oxides, and homemade amorphous-, monoclinic- and tetragonal zirconia prepared from the same Zr source. XRD, XAFS, TG-DTA characterization and surface area measurement were performed. Effects of crystalline phase of ZrO_2 support on selective ethyl acetate production was discussed based on the yields and products ratio (ethyl acetate to sum of C4-alcohols and aldehydes). Based on catalytic performance by 29 kinds of homemade catalysts, amorphous-type ZrO_2 was found to be essentially the most suitable ZrO_2 phase for the selective ethyl acetate formation in cases without any surface modifications. The acid site on the surface of monoclinic-type ZrO_2 catalysts possibly promoted unfavorable acetaldehyde condensation reaction, but addition of Na^+ for poisoning could increase selectivity of ethyl acetate formation. Coordination environment of Cu species for fresh and spent catalysts were discussed.

1. Introduction

Ethyl acetate is an important chemical product that is used as a dilute and extraction solvent, paint, column chromatography, and food additive. It is industrially produced by esterification with a mineral acid such as sulfuric acid, dimerization with an aluminum alcoholate, and acetic acid addition to ethylene with a heteropoly-acid catalyst, end so forth. Recently, from the viewpoint of carbon neutrality and alternative resources to fossil fuels, there have been interest on the production of chemicals and fuels from ethanol [1–3]. The directly synthesis of ethyl acetate by heterogeneous catalyst is one of the reactions and is recognized having advantages as for waste catalyst and separation. It has also been noticed that the only by-product is hydrogen. Direct synthesis from ethanol has been found to be promoted by copper-based catalysts [4–13], and been investigating intensively. Ethyl acetate formation from ethanol is recognized to proceed via acetaldehyde, and the main by-products are butyl alcohol and aldehydes, and dehydration products (Fig. 1).

Ethyl acetate selectivity was found to depend on crystalline phase of zirconia, and monoclinic was reported to be preferred [13]. On the other hand, our trial experiment suggested amorphous phase was better. Recently, Cu-ZrO_2 based catalysts have been attracted considerable interests as CO_2 hydrogenation catalysts to methanol. The crystalline phase dependency of ZrO_2 support has been investigated [14–17]; however, the reported order as for activity and selectivity does not always consistent.

The purpose of this study is to clarify crystalline phase dependency on selective direct ethyl acetate synthesis. It is well known that preparation procedure of a catalyst and trace amount of impurity would effect on the surface property even in the same crystalline phase. Then we prepared ca. 30 kinds of copper-zirconia catalysts with different crystalline phase (amorphous, tetragonal, monoclinic) from the same Zr source, and applied to ethanol conversion. The activity tests of supported Cu catalysts were also examined using representative metal oxides and provided zirconia-based composite oxides.

2. Experimental

2.1. Preparation

Zirconium hydroxide $Zr(OH)_x$ was obtained by hydrolysis of $ZrOCl_2{\cdot}8\,H_2O$ (Nacalai Tesque, GR) with 25 mass% NH_3 aqueous solution at room temperature [18,19]. The final pH value was adjusted to 10, and the aging time was 12 h. The obtained white precipitate was

* Corresponding author.
E-mail address: takashi-yamamoto.ias@tokushima-u.ac.jp (T. Yamamoto).

https://doi.org/10.1016/j.apcatb.2023.122433
Received 1 November 2022; Received in revised form 31 December 2022; Accepted 2 February 2023
Available online 10 February 2023

repeatedly washed with distilled water until Cl^- was not detected by $AgNO_3$ test, dried at 383 K for 12 h, followed by calcination at 573 – 1073 K for 3 h (denoted as ZOH or *x*-Z*y*, where *x* and *y* refer to crystalline phase and the calcination temperature, respectively). The 10 mol % metal-ion doped tetragonal ZrO_2 was prepared by impregnation of ZOH with an aqueous solution of $Y(NO_3)_3{\cdot}nH_2O$ (Wako Pure Chemical) or $Ca(NO_3)_2{\cdot}4\ H_2O$ (Nacalai) at 353 K, followed by calcination at 773 or 873 K (*x*Z*y*, where *x* and *y* refer to kinds of doped metal and the calcination temperature, respectively). The crystalline ZrO_2 without high-temperature calcination was also prepared by hydrothermal treatment of zirconium hydroxide precipitate, with refer to the previous publication by Jung and Bell [20]. Tetragonal ZrO_2 was prepared by hydrothermal treatment of the precipitate, which was obtained by hydrolysis of $ZrOCl_2$ at pH 10, at 453 K for 144 h (ht t-ZrO_2). Monoclinic ZrO_2 was prepared by hydrothermal treatment of the precipitate, which was obtained by hydrolysis of $ZrOCl_2$ at pH 1, at 453 K for 24 h. Unfortunately, hydrothermally synthesized monoclinic ZrO_2 (denoted as ht m-ZrO_2 hereafter) could not be washed by filtration because their particle was too fine. Repeated centrifugal washings did not give Cl^- free ht m- ZrO_2. Then ht m-ZrO_2 was prepared using $ZrO(NO_3)_2{\cdot}2\ H_2O$ (Kishida Chemical, 99%) instead of $ZrOCl_2$. Note that certain amount of weight loss was confirmed in TG-DTA profiles of as-synthesized ht m-ZrO_2 around 673 K (Fig. S1). The prolonged hydrothermal treatment up to 240 h reduced degree of the weight loss, but the loss still existed, indicating that amorphous components may be co-exist. To avoid effect of the possible amorphous phase and increase the crystallinity, it was calcined at 673 K for 10 h.

Supported copper catalysts were prepared by impregnation of a support with an aqueous solution of $Cu(NO_3)_3{\cdot}3\ H_2O$ (Nacalai) at 353 K, followed by calcination under air flow for 3 h in air. Unless otherwise noted, the amount of Cu loading and the calcination temperature were 10 wt% as metal and 673 K, respectively. As the support, homemade ZrO_2 based materials ($Zr(OH)_x$, calcined $Zr(OH)_x$, metal-ion doped ZrO_2, hydrothermally synthesized ZrO_2), provided 15 kinds of zirconia-based catalysts (supplied by Catalysis Society of Japan (Japan Reference Catalyst), and Daiichi Kigenso Kagaku Kogyo Co., LTD (denotes as dkkk)), 13 kinds of metal oxides were utilized. The proved supports used were SiO_2 (JRC-SIO-9A), Al_2O_3 (JRC-ALO-8), TiO_2 (JRC-TIO-6, JRC-TIO-7), niobic acid (JRC-NBO-1), silica-magnesia (JRC-SM-2), amorphous silica–alumina (JRC-SAL-4), MgO (JRC-MGO-3–1000A), CeO_2 (JRC-CEO-2), ZrO_2 (JRC-ZRO-7, −8; and dkkk), amorphous ZrO_2 (JRC-ZRO-6, −9; and dkkk), ZrO_2-based binary oxides (*M*-ZrO_2. *M*: Ca, Y, La, Ce, Ti, W, Si, P and S. dkkk), and CaO (Nacalai, GR). Y_2O_3, La_2O_3 and Nb_2O_5 were obtained by calcination of $Y(NO_3)$, $La(NO_3)_3$ and niobic acid at 773 K for 3 h. $(Ni_{0.1}Cu_{0.9})O$ was prepared by reverse strike co-precipitation method using aqueous solution of nickel and copper nitrates, and tetramethyl ammonium hydroxide, followed by calcination at 1273 K. $CuCr_2O_4$ was prepared by citric acid sol-gel method using copper and chromium nitrates and citric acid. The obtained precursor was finally calcined at 1273 K.

2.2. Characterization

XRD patterns were recorded with a Miniflex diffractometer (Rigaku) equipped with a Ni-filtered Cu Kα radiation source. The N_2 adsorption isotherms at 77 K were measured using a BELSORP-mini (MicrotracBEL). Each sample was outgassed for 2 h before measurement at 573 K or room temperature (as-synthesized samples). The X-ray absorption spectra were recorded with a laboratory-type spectrometer R-XAS Looper (Rigaku) [21] in transmission mode at room temperature. A curved Ge(440) or Ge(220) monochromator crystal was used for the Cu K-edge XANES and EXAFS experiments, respectively. For XANES analysis, the background removal followed by normalization was performed using Igor Pro 6 program [22]. Energy is not calibrated. The data reduction for the EXAFS analysis was performed with the REX2000 program [23]. The radial structure function (RSF) was obtained by Fourier transformation of k^3-weighted EXAFS in the ranges of ca. 3–11.5 $Å^{-1}$. TG-DTA analysis of as-synthesized ZrO_2 supports and supported Cu catalyst precursors was carried out under air flow using a DTG-60 analyzer (Shimadzu) with a heating rate of 10 $K{\cdot}min^{-1}$. Typical profiles were shown in Fig. S1.

2.3. Catalysis

The catalytic test was carried out in a fixed-bed reactor (inner diameter: 8 mm) under atmospheric pressure at 493 K. The ethanol concentration was 20 vol% with N_2 as the balance, and the total flow rate was typically 20 $mL{\cdot}min^{-1}$. The substrate was supplied by a plunger pump N-CL-100 (Nihon Seimitsu Kagaku). Prior to the reaction, 200 mg of each catalyst sample was treated with 50 $mL{\cdot}min^{-1}$ of N_2 flow at 573 K for 2 h. The product distributions were analyzed using three GC-8A gas chromatographs equipped with a flame ionization detector or a TCD. Utilized columns were Gaskuropack 54 (3.0 mm id × 3 m length), PEG-20 M (3.0 mm id × 4 m length) and Active Carbon (3.0 mm id × 2 m length). The conversion, the yield of each product and the selectivity were calculated on the carbon basis at 2 h of the reaction time as follows:

$$Conversion = (moles\ of\ substrate\ reacted) / (moles\ of\ substrate\ loaded) \times 100\%$$

$$Yield = (carbon\ in\ given\ product) / (carbon\ loaded\ in\ substrate) \times 100\%$$

3. Results

3.1. Structural analysis

3.1.1. XRD

Fig. 2 shows typical XRD patterns of as-synthesized zirconium hydroxide and ZrO_2-based supports. As-prepared zirconium hydroxide was amorphous, and was crystalized to monoclinic phase by calcination

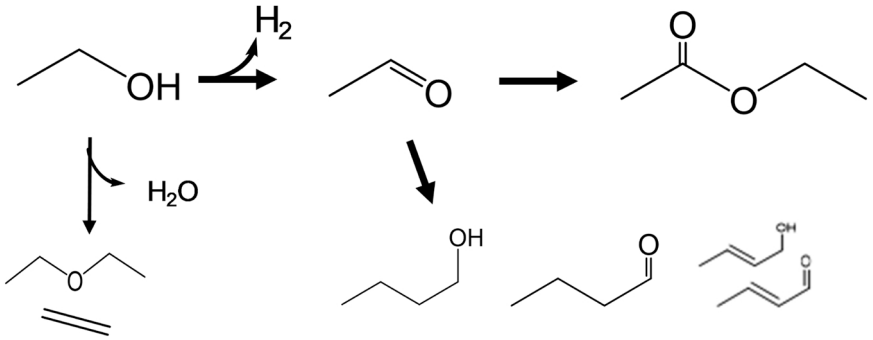

Fig. 1. Possible reaction pathway of ethanol conversion.

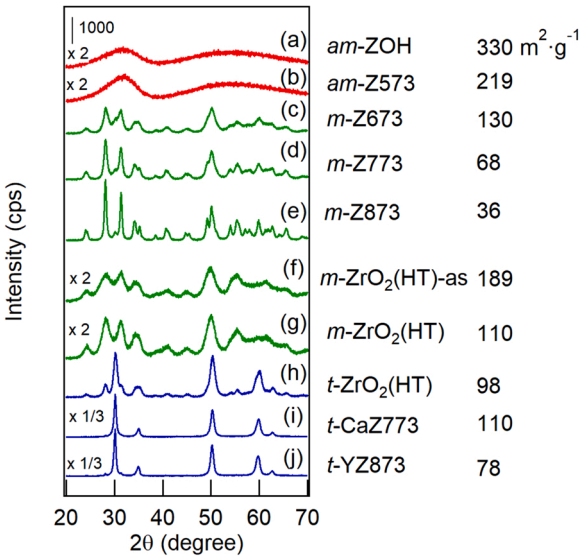

Fig. 2. XRD patterns of ZrO_2-based materials and the surface area: (a) as-synthesized $Zr(OH)_x$, calcined at (b) 573, (c) 673, (d) 773 and (e) 873 K, (f) hydrothermally synthesized monoclinic ZrO_2 and (g) the calcined one at 673 K, (h) hydrothermally synthesized tetragonal ZrO_2, (i) Ca-doped ZrO_2 calcined at 773 K, and (j) Y-doped ZrO_2 calcined at 873 K.

above 673 K. Small fraction of tetragonal ZrO_2 phases was co-exist. Crystalline phases of Ca- and Y-doped ZrO_2 were tetragonal and/or cubic. It has been reported that hydrothermal treatment of zirconium hydroxide would give crystallized zirconia, the crystalline phase of which could be controlled as tetragonal or monoclinic by choosing pH of a mother liquid at the hydrolysis [20,24,25]. We could obtain monoclinic and tetragonal ZrO_2 by hydrothermal treatment as same as the previous publication. Diffraction lines of the as-synthesized ht m-ZrO_2 was sharpened after calcination at 673 K.

Using these zirconia, supported copper catalysts were prepared by conventional impregnation method followed by calcination. Fig. 3 shows XRD patterns of typical supported Cu catalysts. In cases $Zr(OH)_x$ was utilized as the support, the catalyst calcined at 673 K was X-ray amorphous. Cu-related crystalline phase was not detected. Tetragonal ZrO_2 phase appeared after calcination of $Cu/Zr(OH)_x$ precursor at 773 – 873 K. Crystalline phases of other catalysts related to ZrO_2 kept after Cu-loading procedure. Diffraction lines due to crystalline CuO species were detected on most of monoclinic and tetragonal ZrO_2 supported catalysts.

Fig. 4 shows XRD patterns of spent catalyst after ethanol conversion at 673 K. Trace levels of diffraction lines due to metallic copper were confirmed on amorphous catalysts. Distinct diffraction lines due to metallic copper were detected for almost of the catalysts where Cu loading were more than 3 wt%. Diffraction lines due to CuO observed on the fresh catalysts were diminished.

3.1.2. XAFS

To investigate local structure around Cu in fresh and spent catalysts, XANES and EXAFS characterization was carried out. Fig. 5 shows Cu K-edge EXAFS spectra of fresh catalysts and the radial structure functions (RSFs) obtained by Fourier transformation of the EXAFS functions. The intense peak around 1.5 Å shown in all RSFs was due to Cu-O pair for the first coordination sphere. RSFs of some Cu-ZrO_2 catalysts in which crystalline CuO phases were detected in their XRD patterns gave distinct additional peaks above 2 Å, resemble to that of CuO. In cases for $Zr(OH)_x$ was used for catalyst supports and/or Cu loadings were less than 3 wt%, distinct peaks were not confirmed around in these region.

Fig. 6 shows Cu K-edge XANES spectra of reference Cu^{2+} compounds with different coordination symmetry. $CuCr_2O_4$ contains tetrahedral CuO_4 species, and gave a characteristic preedge peak around 8975 eV. But the peak intensity is small because Cu^{2+} is d^9 [26]. $(Ni_{0.9}Cu_{0.1})O$ with NaCl structure [27] did not gave any characteristic structure below 8995 eV. A shoulder could be seen around 8985 eV in cases the symmetry of a Cu polyhedron is distorted from O_h such as $Cu(OH)_2$. The

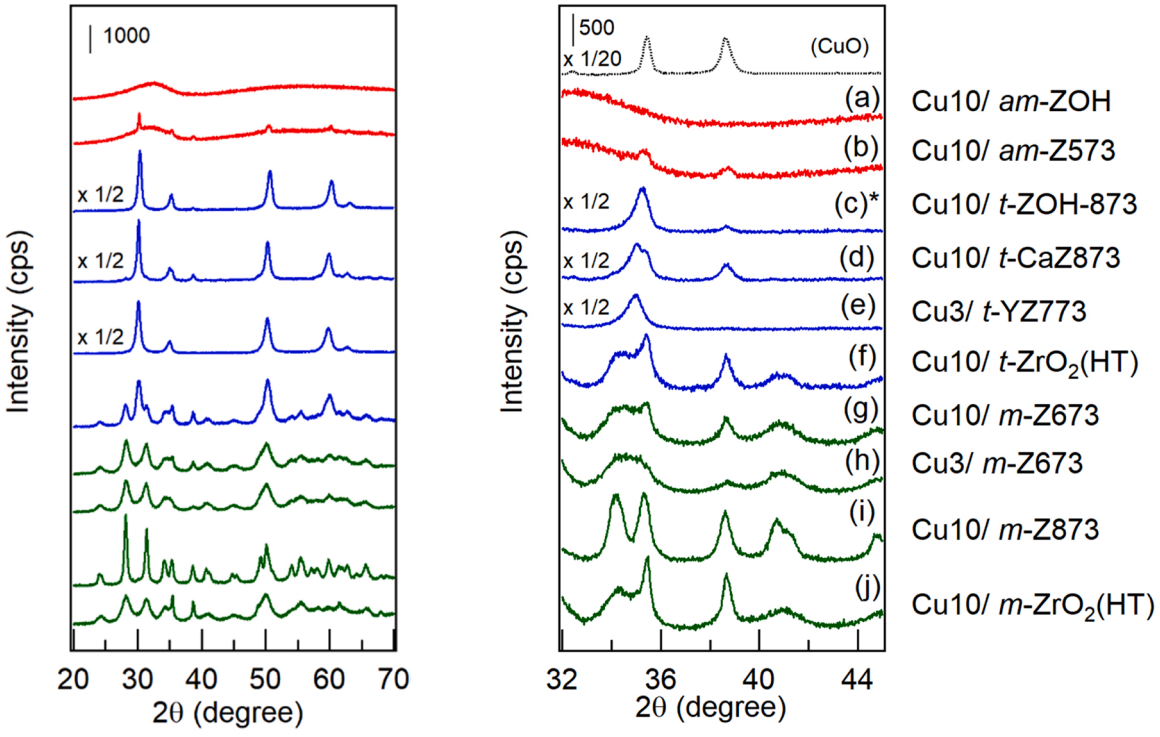

Fig. 3. XRD patterns of supported Cu catalysts on (a) $Zr(OH)_x$ (*am*-ZOH), (b) calcined ZOH at 573 K (*am*-Z573), (c) ZOH* , (d) Ca-ZrO_2 calcined at 873 K (*t*-CaZ873), (e) Y-ZrO_2 calcined at 773 K (*t*-YZ773), (f) hydrothermally synthesized tetragonal ZrO_2 (*t*-ZrO_2(HT)), (g)-(h) ZOH calcined at 673 K (*m*-Z673), (i) ZOH calcined at 873 K (*m*-Z873), and (j) hydrothermally synthesized monoclinic ZrO_2 (*m*-ZrO_2(HT)). Cu: 10 wt%; catalyst calcination temperature: 673 K (*873 K).

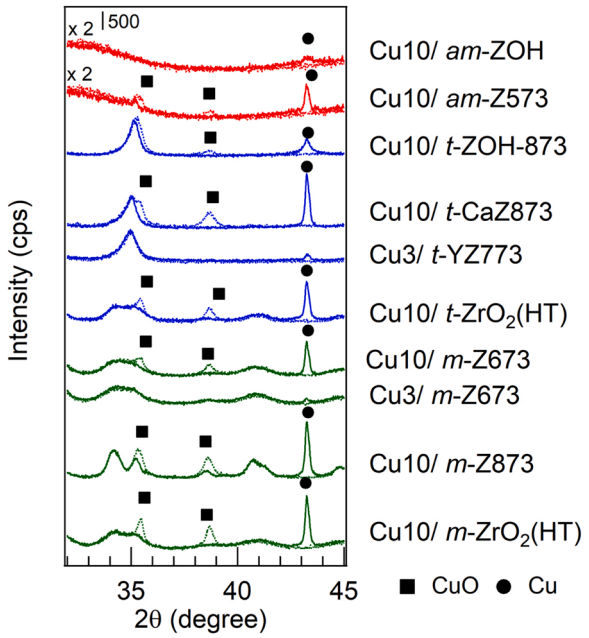

Fig. 4. XRD patterns of spent and fresh Cu-ZrO_2 catalysts. Solid line: spent catalyst; dashed line: fresh catalyst. Catalyst: see Fig. 3.

shoulder position shifted towards lower energies as it approaches the D_{4h} symmetry. Basic copper hydroxide $Cu(OH)_2{\cdot}CuCO_3{\cdot}H_2O$ possess CuO_6 unit, the unit of which is quite distorted and far from O_h symmetry. The shoulder does not present in the XANES spectrum.

Fig. 7 shows Cu K-edge XANES spectra of homemade ZrO_2 supported Cu catalysts before and after activity test. The apparent absorption edge position for fresh catalysts was identical to that of divalent copper compounds. The spectral configurations of catalysts supported on crystalized monoclinic or tetragonal ZrO_2 were similar to that of CuO with a shoulder around 8985 eV. Any distinct shoulder was not confirmed in the spectra for amorphous catalysts.

The absorption edge of the present catalysts shifted to lower energy after catalytic test, and confirmed to be similar to that of metallic copper. The edge-shift was small for only spent Cu10/*am*-ZOH catalyst. This spectrum could be reproduced by summation of 25% metal and 75% fresh catalyst, as shown in Fig. S2. The Cu10/*am*-Z573 catalyst is X-ray amorphous as shown in Fig. 3. The XANES spectrum of the spent catalyst was similar to that of Cu foil, the fraction of which was estimated to be ca. 2/3 by convolution analysis.

3.2. Activity test

3.2.1. Metal-oxide support

First, we performed activity tests using various metal oxide catalysts. Results are shown in Fig. 8 and Table 1. The product distributions were also summarized in Tab. S1 in more detail. Acetaldehyde was the primary and main product. It has been recognized that saturated/unsaturated C4-aldehydes and alcohols (C4-al,ol) and ethyl acetate (AcOEt) formation from ethanol would proceed via acetaldehyde by different pathway, as shown in Fig. 1. Then the product ratio AcOEt / C4-al,ol was shown as the selectivity index. As same as previous studies, ethyl acetate was formed by Cu-ZrO_2 catalyst, but small for other supports. The ethyl acetate yield and the selectivity ratio for $Zr(OH)_x$ support (Entry 11) was superior to that for monoclinic ZrO_2 (Entry 12). In cases for MgO and CaO of typical solid bases (Entry 9, 10), only acetaldehyde was produced. Y_2O_3 and La_2O_3 of rare earth oxides are expected to have both acid and base sites like ZrO_2 [28–33]. However, ethyl acetate yield was scarce. Any effective supports suitable for the direct ethyl acetate synthesis were not found among these catalysts examined.

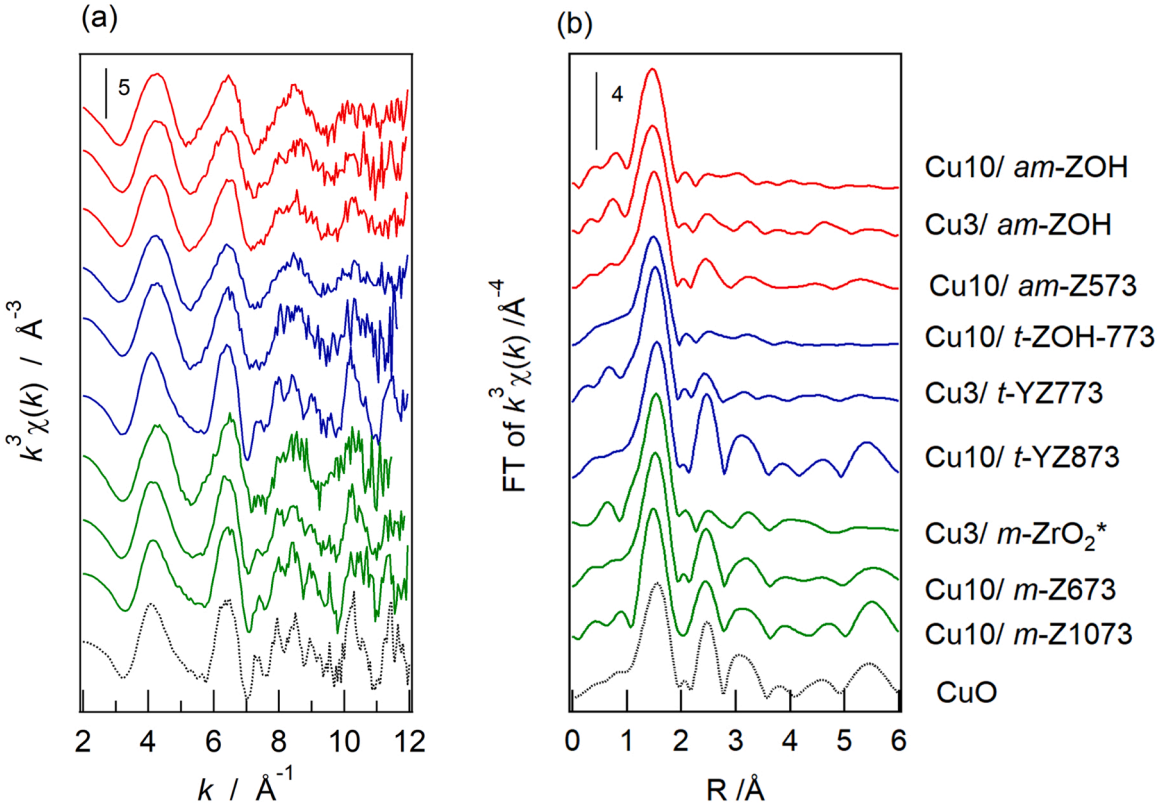

Fig. 5. Cu K-edge EXAFS spectra (a) of fresh Cu-ZrO_2 catalysts and the Fourier transforms (b). * JRC-ZRO-7.

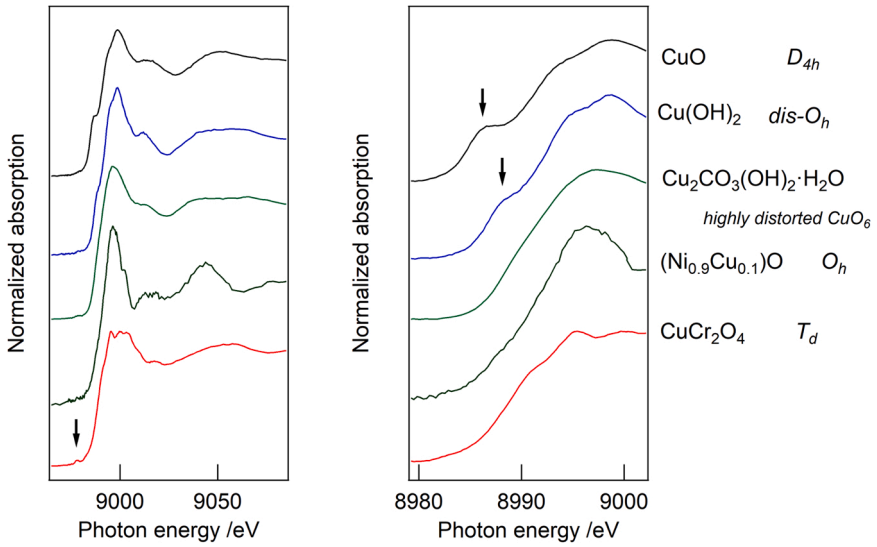

Fig. 6. Cu K-edge XANES spectra of reference Cu^{2+} compounds with different coordination symmetry.

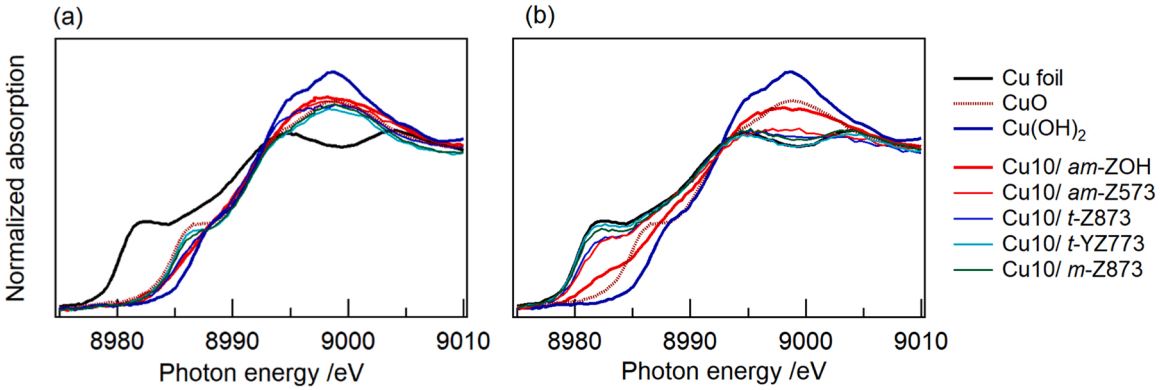

Fig. 7. Cu K-edge XANES spectra of fresh (a) and spent Cu-ZrO_2 catalysts (b).

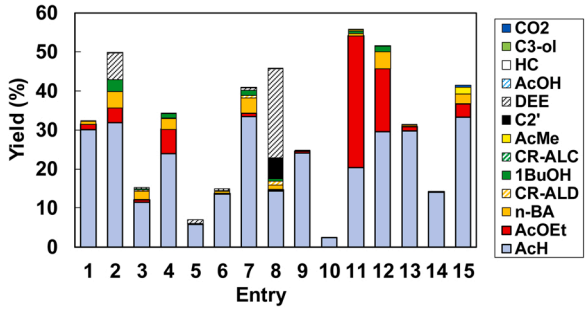

Fig. 8. Results of ethanol conversion over metal oxide supported Cu catalysts. Catalyst: see Table 1, 10 wt% as Cu, 200 mg; ethanol: 20%; N_2: balance; total flow rate: 20 mL·min^{-1}; 493 K; 1 atm. AcH: acetaldehyde; AcOEt: ethyl acetate; n-BA: 1-butyl aldehyde; CR-ALD: croton aldehyde; 1BuOH: 1-butanol; CR-ALC: crotyl alcohol; AcMe: acetone; C2′: ethene; DEE: diethyl ether; AcOH: acetic acid; HC: sum of C2-C4 hydrocarbons; C3-ol: propanols; C4-al,ol: sum of saturated/unsaturated C4 alcohols and aldehydes.

3.2.2. *Provided ZrO_2-based support*

As shown above, ZrO_2 was re-confirmed to be suitable support of Cu for direct ethyl acetate synthesis from ethanol. Next, screening of ZrO_2-based materials for Cu support in ethanol conversion was carried out using 15 kinds of provided materials. Fig. 9, Table 2 and S2 summarize the results. Ethyl acetate formation could be promoted by all these catalysts, and the yields were higher by ZrO_2 alone without any additives. It should be noted that yields of undesirable by-products except for acetaldehyde; mainly n-butyl aldehyde and 1-butyl alcohol; were small for amorphous $Zr(OH)_x$ supported catalysts. The WO_3, SiO_2, PO_4^-, and SO_4^{2-}-containing catalysts (Entry 25–28), which might exhibit solid acidity, gave C4-al,ol compounds much more than ethyl acetate. Most of the produced alcohols and aldehydes were saturated compounds for all catalysts examined in the present study.

3.2.3. *Homemade ZrO_2-based support*

Next, we performed activity test with homemade ZrO_2 support prepared from the same Zr source. Fig. 10, Table 3, S3 summarized the results for each crystalline phase of ZrO_2. In cases ZrO_2 support was X-ray amorphous (Fig. 10(a)), ethyl acetate formation was promoted effectively. Other products except for acetaldehyde and ethyl acetate were scarce. The selective index (AcOEt / C4-al,-ol ratio) were as high as around 10. As shown in Fig. 11, the catalytic activity of an amorphous-type catalyst slightly decreased with time on stream, but the selective index did not change after 24 h. The amorphous catalyst prepared from $ZrO(NO_3)_2$ exhibited the identical catalytic performance (Entry 33) as a catalyst prepared from $ZrOCl_2$ source (Entry 32). The present homemade monoclinic-type catalysts promoted ethyl acetate formation, but the yields were much less than those for amorphous type catalysts (Fig. 10 (b)). The C4-alcohol and aldehyde production was promoted so much, resulting that products ratio for ethyl acetate formation was almost one-tenth comparing to that of amorphous-types. Tetragonal-type catalysts

Table 1
Results of ethanol conversion over Cu catalysts supported on metal oxides.

Entry	Support		Area $m^2 \cdot g^{-1}$	Conv.(%)	Yield (%) AcH	AcOEt	C4-al,ol	Others	Ratio[c]
1	SiO_2		261	32.3	30.0	1.4	0.8	0.0	1.8
2	γ-Al_2O_3		154	49.8	31.8	3.9	7.2	6.9	0.5
3	TiO_2	*anatase*	107	15.2	11.5	0.7	2.8	0.2	0.2
4	TiO_2	*rutile*	68	34.2	23.9	6.3	4.0	0.0	1.6
5	$Nb_2O_5 \cdot nH_2O$		105	7.0	5.9	0.0	0.0	1.1	
6	Nb_2O_5	*TT-phase*	53	14.9	13.6	0.1	0.6	0.5	0.2
7	SiO_2-MgO		414	40.8	33.4	0.9	5.9	0.6	0.2
8	SiO_2-Al_2O_3		336	45.7	14.3	0.4	2.7	28.3	0.2
9	MgO		63	24.7	24.1	0.4	0.2	0.1	1.9
10	CaO		7	2.5	2.5	0.0	0.0	0.0	
11	$Zr(OH)_x^a$	(am-1)	172	55.7	20.4	33.7	1.3	0.3	26
12	ZrO_2^b	(m-1)	95	51.6	29.6	16.1	5.7	0.2	2.8
13	Y_2O_3		13	31.3	29.8	1.1	0.3	0.1	3.6
14	La_2O_3		7	14.2	14.0	0.2	0.0	0.0	
15	CeO_2		106	41.6	33.2	3.4	2.5	2.4	1.4

Catalyst: 10 wt% as Cu, 200 mg; ethanol: 20%; N_2: balance; total flow rate: 20 mL·min^{-1}; 493 K; 1 atm. Substrate: see Fig. 8.
[a]JRC-ZRO-6, [b]JRC-ZRO-7, [c] AcOEt / C4-al,ol.

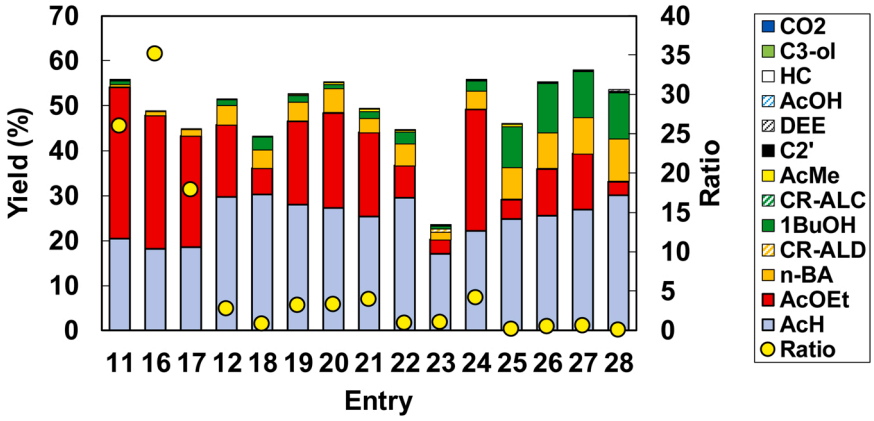

Fig. 9. Results of ethanol conversion over available ZrO_2-based oxide supported Cu catalysts. Catalyst: see Table 2, 200 mg; ethanol: 20%; N_2: balance; total flow rate: 20 mL·min^{-1}; 493 K; 1 atm. Substrate: see Fig. 8. Ratio: ethyl acetate / C4-al,ol.

Table 2
Results of ethanol conversion over provided ZrO_2-based materials supported Cu catalysts.

Entry	Catalyst	wt%[h]	Area $m^2 \cdot g^{-1}$	Conv. (%)	Yield (%) AcH	AcOEt	C4-al,ol	Others	Ratio[i]
11	am-1[a,b]	-	172	55.7	20.4	33.7	1.3	0.3	26
16	am-2[a,c]	-	194	48.8	18.1	29.6	0.8	0.2	35
17	am-3[a,d]	-	221	44.7	18.6	24.7	1.4	0.1	18
12	m-1[e,f]	-	95	51.6	29.6	16.1	5.7	0.2	2.8
18	m-2[e,g]	-	20	43.0	30.3	5.8	6.9	0.0	0.8
19	m-3[d,e]	-	89	52.5	27.9	18.6	5.8	0.2	3.2
20	CaO-ZrO_2^d	2	89	55.2	27.2	21.2	6.3	0.4	3.4
21	Y_2O_3-ZrO_2^d	14	82	49.2	25.4	18.6	4.6	0.5	4.1
22	La_2O_3-ZrO_2^d	9	65	44.6	29.5	7.1	7.6	0.4	0.9
23	CeO_2-ZrO_2^d	50	49	23.5	17.0	3.2	3.0	0.3	1.1
24	TiO_2-ZrO_2^d	20	167	55.7	22.1	27.1	6.4	0.1	4.2
25	WO_3-ZrO_2^d	10	106	46.0	24.7	4.4	16.1	0.7	0.3
26	SiO_2-ZrO_2^d	10	159	55.1	25.6	10.3	19.1	0.1	0.5
27	PO_4-ZrO_2^d	8	161	57.8	26.8	12.4	18.4	0.2	0.7
28	SO_4-ZrO_2^d	3	102	53.5	30.1	3.0	20.0	0.4	0.1

Catalyst: 200 mg; ethanol: 20%; N_2: balance; total flow rate: 20 mL·min^{-1}; 493 K; 1 atm. Substrate: see Fig. 8.
[a] X-ray amorphous, [b] JRC-ZRO-6, [c] JRC-ZRO-9, [d] dkkk, [e] monoclinic ZrO_2, [f] JRC-ZRO-7, [g] JRC-ZRO-8, [h] as metal oxide,
[i] AcOAc / C4-al,ol

also promoted ethyl acetate formation, and the yields and the selective index were less than those for amorphous-type catalysts. Overall, the selective index was generally found to independent of loading amount of Cu and calcination temperature of catalyst among the same crystalline phase of ZrO_2 support.

In the present study, we examined catalytic performance of 29 kinds of home-made ZrO_2 catalysts. The loading amounts, surface area, and the ethanol conversions were wide ranging. Then to help comparison of catalytic properties based on crystalline phase, yields of three core compounds were plotted as a function of ethanol conversion (Fig. 12).

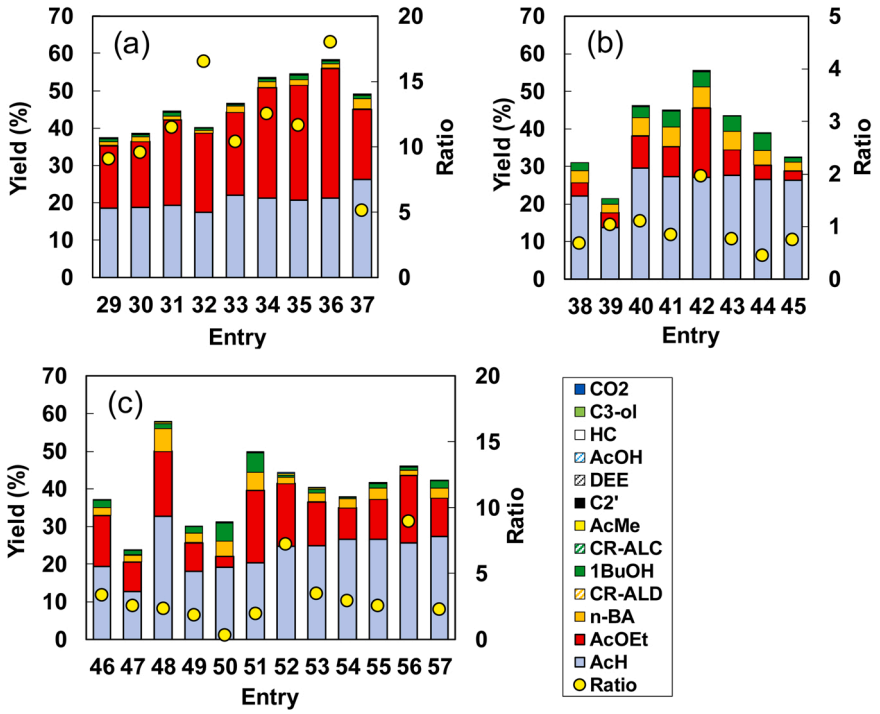

Fig. 10. Results of ethanol conversion over homemade ZrO_2 supported Cu catalysts. Crystalline phases of ZrO_2: amorphous (a), monoclinic (b), and tetragonal (c). Catalyst: see Table 3, 200 mg; ethanol: 20%; N_2: balance; total flow rate: 20 mL·min^{-1}; 493 K; 1 atm. Substrate: see Fig. 8. Ratio: ethyl acetate / C4-al,ol.

As shown in Fig. 12(a), ethyl acetate yields for amorphous-type catalysts were higher than that for monoclinic-type at the similar conversion level. Yields for tetragonal-type catalysts were the intermediate. The amount of C4 alcohols and aldehydes produced by amorphous catalysts were less than others. Other remarkable differences were not confirmed. Note that the effect of contact time on the product distribution was examined for an amorphous-type catalyst. The lower contact time (lower GHSV) little influenced on the selective index as shown in Fig. 13.

Finally, the selective index was summarized as a function of ethanol conversion and apparent surface density of Cu atoms (Fig. 14). It is obvious that amorphous-type catalysts exhibited higher selective index much more than those for monoclinic- and tetragonal-type catalysts independent of conversion level and surface density.

4. Discussion

4.1. Structure

TG-DTA profiles shown in Figs. S1 suggest that amorphous $Zr(OH)_x$ was crystalized by calcination around 673 K, whereas impregnation of 3–10 wt% Cu species onto $Zr(OH)_x$ raise the crystallization temperature by ca. 80 K to form metastable tetragonal phase. The crystal phase of Cu-ZrO_2 catalysts could be controlled as tetragonal or amorphous by choice of calcination temperature of Cu-ion impregnated $Zr(OH)_x$ precursor, as similar to the previous study [16,17]. In addition, we prepared tetragonal-type catalysts by other two methods in the present study; i.e., (1) doping Ca or Y ions to $Zr(OH)_x$ and calcination in advance, (2) hydrothermal treatment of $Zr(OH)_x$ precipitate. Higher temperature calcination of $Zr(OH)_x$ above 673 K or hydrothermal treatment of Zr $(OH)_x$ at low pH gave monoclinic-type ZrO_2. As a brief summary of the catalyst preparation, we could prepare Cu-ZrO_2 catalysts with different crystalline phases of ZrO_2 (amorphous, tetragonal, monoclinic) from the same Zr source material by multiple methods.

Here, local structure of Cu species in Cu10/am-ZOH catalyst (10 wt% Cu/$Zr(OH)_x$ calcined at 673 K) would be discussed. The surface area of as-synthesized $Zr(OH)_x$ is as large as 330 m^2·g^{-1}, and reduced to 1/3 by calcination at 673 K in dependently of metal-ion addition. XRD and XAFS characterization of Cu10/am-ZOH catalyst clearly show that Cu species does not form CuO aggregate, but are atomically dispersed. Color of the catalyst is greenish brown. We have reported that substitutional-type solid solution could be formed in Ga-ZrO_2 [34] and Yb(Y)-ZrO_2 [19] prepared in the similar procedure. Then we suppose the copper species is incorporated inside the bulk during catalyst preparation in highly dispersed form, and form solid solution, as proposed by Tada [17].

It has been reported that CuO-ZrO_2 solid solution could be formed up to 20 mol% by co-precipitation procedure [35,36]. Because ionic radius of Cu^{2+} (0.73 Å, 6-fold coordination) is similar to that of Zr^{4+} (0.72 Å) [37], substitutional solid solution could be formed. However, distinct Cu-(O)-Zr pairs were not observed in the RSF (Fig. 5), as same as the previous study [17,38]. The oxidation number of the added copper ions is lower than that of the zirconium ions. As with many zirconia-based solid solutions, it is assumed that oxygen vacancy is present to maintain electrical neutrality. We speculate resulting large local distortion would drastically reduce the Cu-(O)-Zr contributions in Cu K-edge EXAFS oscillations. The spectral features of Cu K-edge XANES spectra of fresh Cu10/am-ZOH is not the same as those of reference compounds shown in Fig. 7. Based on absence of remarkable pre-edge peaks and shoulder around 8985 eV, we suppose Cu species in fresh Cu10/am-ZOH exist as quite distorted CuO_6 polyhedral species atomically dispersed inside ZrO_2 bulk forming solid solution. XRD and XAFS characterization showed that copper species in Cu10/am-ZOH were reduced to metallic copper after catalytic test, while 3/4 of copper species in spent catalyst remained unchanged, the value of which was evaluated by XANES spectrometry. In cases 573 K-calcined $Zr(OH)_x$ was used as the support, 10 wt% Cu-loaded catalyst calcined at 673 K was X-ray amorphous. Fraction of reduced species in the spent catalyst was evaluated to be 2/3. It shows copper species near the surface were readily reduced, while those atomically dispersed inside the bulk were not.

In cases monoclinic or tetragonal zirconia was used, surface area of the Cu-supported catalyst also reduced during their preparation procedure. But the decrease degree was only about 20% at maximum,

Table 3
Results of ethanol conversion over homemade ZrO_2-based materials supported Cu catalysts.

(a) Amorphous-type

Entry	Catalyst	wt%	Area $m^2 \cdot g^{-1}$	Conv.(%)	Yield (%) AcH	AcOEt	C4-al,ol	Others	Ratio[c]
29	am-4	2.6	134	37.2	18.5	16.8	1.9	0.1	9.1
30	am-5	3	172	38.4	18.7	17.7	1.8	0.2	9.6
31	am-6	5.3	173	44.3	19.3	22.9	2.0	0.1	11
32	am-7	10	150	40.1	17.4	21.2	1.3	0.1	17
33	am-8[a]	10	120	46.5	22.0	22.2	2.1	0.2	10
34	am-9[b]	10	186	53.4	21.2	29.6	2.4	0.2	13
35	am-10	11	178	54.4	20.7	30.8	2.6	0.2	12
36	am-11	17	172	58.3	21.2	34.9	1.9	0.3	18
37	am-12	23	65	49.1	26.2	18.9	3.7	0.3	5.1

[a] $Zr(OH)_x$ calcined at 573 K, [b] prepared from $ZrO(NO_3)_2$, [c] AcOEt / C4-al,ol

(b) Monoclinic-type

Entry	Catalyst	temp. / K[b]	wt%	Area $m^2 \cdot g^{-1}$	Conv.(%)	Yield (%) AcH	AcOEt	C4-al,ol	Others	Ratio[c]
38	m-4	773	1	65	30.9	22.1	3.6	5.3	0.0	0.7
39	m-5[a]	673	1	113	21.4	13.8	3.9	3.7	0.0	1.0
40	m-6	773	3	63	45.9	29.6	8.5	7.7	0.1	1.1
41	m-7	673	3	106	44.9	27.3	8.0	9.5	0.1	0.8
42	m-8	673	10	100	55.3	27.0	18.6	9.5	0.2	2.0
43	m-9[a]	673	10	89	43.4	27.7	6.8	8.9	0.1	0.8
44	m-10	873	10	31	38.8	26.6	3.8	8.4	0.0	0.4
45	m-11	1073	10	13	32.2	26.3	2.5	3.4	0.0	0.7

[a] hydrothermally synthesized ZrO_2, [b] calcination temperature of $Zr(OH)_x$ precursor, [c] AcOEt / C4-al,ol

(c) Tetragonal-type

Entry	Catalyst	Support	wt%	area $m^2 \cdot g^{-1}$	Conv.(%)	Yield (%) AcH	AcOEt	C4-al,ol	Others	Ratio[f]
46	t-1	$Zr(OH)_x$[a]	3	127	37.0	19.4	13.5	4.0	0.0	3.4
47	t-2	$Zr(OH)_x$[b]	3	162	23.7	12.8	7.8	3.1	0.0	2.5
48	t-3[c]	ZOH	10	42	57.7	32.8	17.2	7.4	0.4	2.3
49	t-4[d]	ZOH	10	46	30.0	18.1	7.7	4.2	0.1	1.8
50	t-5	t-ZrO_2[e]	1	89	31.1	19.2	3.0	8.9	0.0	0.3
51	t-6	t-ZrO_2[e]	10	86	49.8	20.3	19.4	9.9	0.2	1.9
52	t-7	Y-ZrO_2[c]	3	82	44.5	24.8	16.6	2.3	0.8	7.2
53	t-8	Y-ZrO_2[c]	10	77	40.2	24.9	11.7	3.4	0.3	3.5
54	t-9	Y-ZrO_2[d]	10	36	37.9	26.6	8.4	2.8	0.1	2.9
55	t-10	Ca-ZrO_2[c]	3	80	41.5	26.5	10.7	4.2	0.1	2.6
56	t-11	Ca-ZrO_2[c]	10	83	46.0	25.7	18.0	2.0	0.4	9.0
57	t-12	Ca-ZrO_2[d]	10	49	42.2	27.4	10.2	4.4	0.2	2.3

Catalyst: 200 mg; ethanol: 20%; N_2: balance; total flow rate: 20 mL·min^{-1}; 493 K; 1 atm. Substrate: see Fig. 8.
[a] Calcined at 573 K, [b] prepared from $ZrO(NO_3)_2$, [c] calcined at 773 K, [d] calcined at 873 K, [e] hydrothermally synthesized tetragonal ZrO_2, [f] AcOEt / C4-al,ol

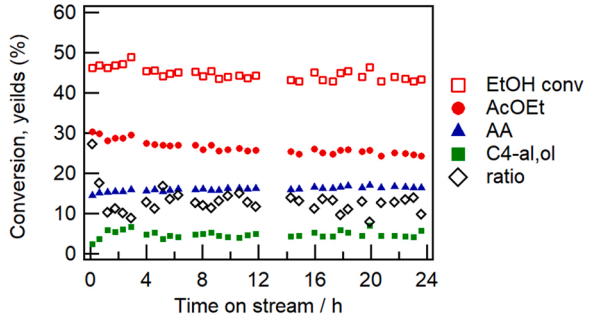

Fig. 11. Ethanol conversion and products yield with the reaction time over amorphous-type catalyst. Catalyst: am-10 (see Table 3), 200 mg; ethanol: 20%; N_2: balance; total flow rate: 20 mL·min^{-1}; 493 K; 1 atm. Substrate: see Fig. 8. Ratio: ethyl acetate / C4-al,ol.

indicating that Cu species located mainly on the surface. Formation of CuO crystallite could be detected by XRD at the apparent surface density more than 2 atom·nm^{-2}. There aggregated species were easily reduced to metallic copper after catalytic test.

4.2. Effect of crystalline phase of ZrO_2

As summarized in Figs. 10, 12, and 14, activity test of ethanol conversion was done systematically over Cu-ZrO_2 catalysts prepared from the same Zr source. We could find clear evidence that amorphous-type catalyst exhibited the highest selective index for direct ethyl acetate synthesis from ethanol. The order of suitable crystalline phase was found to be as follows; amorphous > > tetragonal > monoclinic. The present 8 kinds of monoclinic-type catalysts promoted undesirable C4-alcohols/aldehydes formation preference to ethyl acetate formation under the present reaction condition, except for one exception. Our result was not consistent with the crystalline phase dependency reported previously (monoclinic ≥ amorphous > tetragonal) [13]. One possible reason for this discrepancy among our results and their study might be the source of ZrO_2. In their study, the sources of ZrO_2 for different crystalline phase are noted not to be the same. Here, we focus on the selectivity index ratio for monoclinic-type catalysts shown in Tables 2 and 3. The homemade catalysts gave similar values, whereas the deviations are larger for the provided ones. It shows differences in some preparation procedures and/or Zr sources might be responsible for differences in their catalytic property even in the same crystalline phases detecdted.

It has been reported that ZrO_2 could promote vapor phase aldol condensation of acetaldehyde at 573 K [39]. In the zirconium-based catalyzed ethanol conversion to 1,3-butadiene, it has been reported that the aldol condensation of acetaldehyde could be promoted by Lewis acid sites due to zirconium cation [40,41]. Aldol condensation reaction is known to be promoted by both acid and base sites. In the present study, typical solid base supported Cu catalysts (MgO, CaO, La_2O_3) promoted acetaldehyde formation, but little for C4-al,ol formation. Then the present reaction condition such as pretreatment and/or reaction

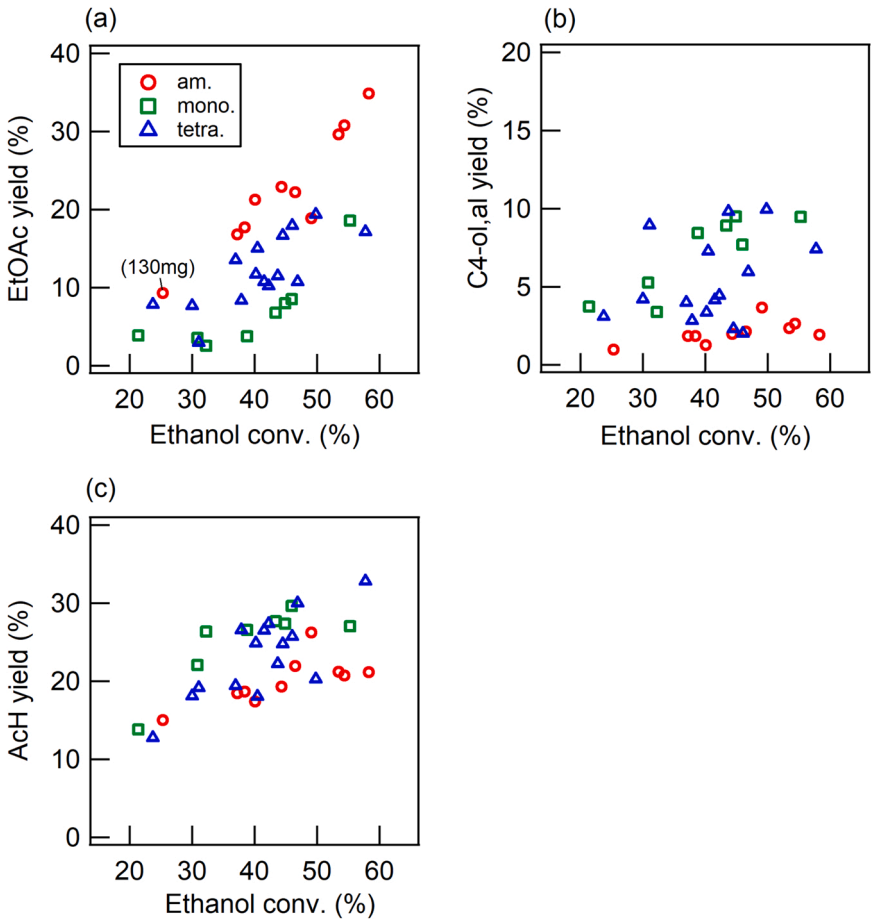

Fig. 12. Comparison of product yields at the same ethanol conversion level over homemade ZrO_2 supported Cu catalysts with different crystalline phase. Ethyl acetate: (a); sum of saturated/unsaturated C4 alcohols and aldehyde: (b); acetaldehyde (c). Catalyst: 200 mg; ethanol: 20%; N_2: balance; total flow rate: 20 mL·min^{-1}; 493 K; 1 atm.

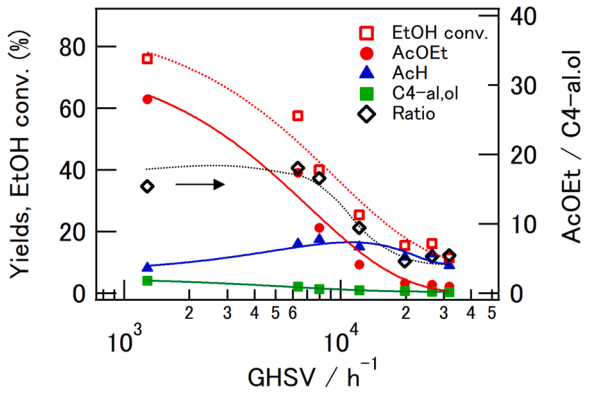

Fig. 13. Contact time dependency on ethanol conversion over amorphous-type catalyst. Catalyst: am-17 (see Table 3), 50 – 1000 mg; ethanol: 20%; N_2: balance; total flow rate: 20 mL·min^{-1}; 493 K; 1 atm. Substrate: see Fig. 8. Ratio: ethyl acetate / C4-al,ol.

temperature was not enough for base-catalyzed condensation reaction. Pokroveski reported that Lewis acidity of monoclinic zirconia is higher than that of tetragonal zirconia based on CO/CO_2 adsorption experiments [42]. Yamamoto reported that monoclinic ZrO_2 exhibit stronger acidity than tetragonal one, and exhibited higher catalytic performance for selective 1,4-butanediol dehydration [43]. As shown in Fig. 9, WO_3-, SiO_2, PO_4-, and SO_4^{2-}-containing catalysts (Entry 25–28) gave C4-al,ol compounds much more than ethyl acetate. We speculate the present C4-al,ol formation could be promoted by acid site on the surface, resulting from the catalyst composition.

We propose here that C4-al,ol formation confirmed in the present ethyl acetate synthesis over Cu-ZrO_2 would be promoted by acid site on the surface via condensation of acetaldehyde. Monoclinic ZrO_2 possess strong Lewis acid site intrinsically effective for the condensation, whereas catalytic performance of amorphous-type catalyst is not enough for the promotion. Tetragonal-type catalysts also possess active site for acetaldehyde condensation, but the activity is inferior to that of monoclinic-type catalyst. Based on this assumption, it is expected that suppressing the acidity of monoclinic-type catalyst would improve ethyl acetate selectivity, while promoting acidity to amorphous-type catalysts would decrease the selectivity. It has been reported that addition of Na^+ to ZrO_2 would decrease the acid amount, and could control the catalytic performance for alcohols dehydration [43,44]. We have examined catalysis of metal-ion doped ZrO_2 for 2-butanol decomposition, and confirmed that B-ZrO_2 promotes typical acid catalyzed reaction to form 2-butenes [34]. $CuSO_4$ and the calcined ones is reported to exhibit solid acidity [28,45]. To confirm contribution of acid site of Cu-ZrO_2 catalysts on product distributions in ethyl acetate synthesis, Na^+, BO_3^- and SO_4^{2-} co-doped catalysts were prepared, and activity test were carried out. Other amorphous-type catalysts were also prepared using 3 kinds of copper salt. The list of prepared acidity- and basicity-modified catalysts and results of ethanol conversion are summarized in Table 4. As expected, Na^+ addition to monoclinic-type catalyst suppressed C4-al,ol formation, and increased ethyl acetate / C4-al,ol ratio by ca. 4 times. Attempts to add acidic character on the surface of amorphous-type catalysts increased yields of C4-al,ol. compounds. The ethyl acetate

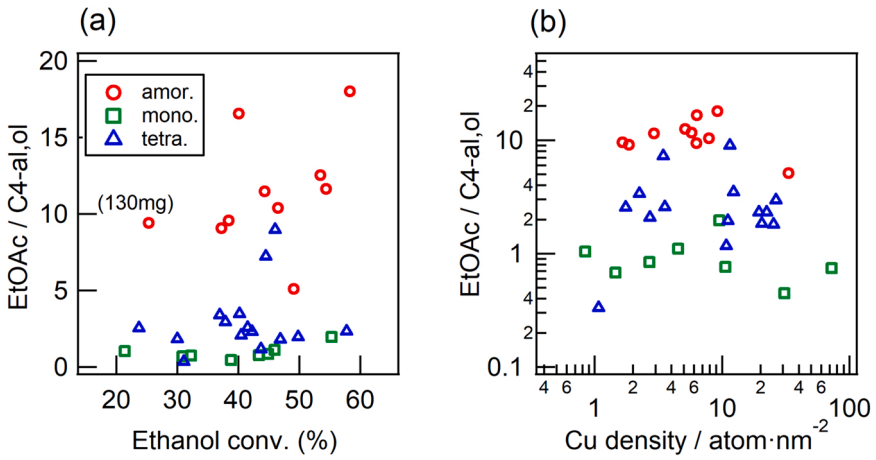

Fig. 14. Crystalline phase dependency of ZrO_2 support on ethil acetate formation selectivity summaried as a function of (a) ethanol conversion, and (b) apparent Cu density.

Table 4
Ethanol conversion over acidity- or basicity modified Cu-ZrO_2 catalysts.

Entry	Support	Cu source[a]	Additive		Conv.(%)	Yield (%)				Ratio[f]
				wt%		AcH	AcOEt	C4-al,ol	Others	
42	m-ZrO_2	$Cu(NO_3)_2$	-		55.3	27.0	18.6	9.5	0.2	2.0
58	(ZOH673)	$Cu(NO_3)_2$	$NaNO_3$	1[b]	45.4	32.3	10.4	1.3	1.4	7.9
18	m-ZrO_2	$Cu(NO_3)_2$	-		43.0	30.3	5.8	6.9	0.0	0.8
59	(JRC-ZRO8)	$Cu(NO_3)_2$	$NaNO_3$	0.1[b]	41.6	30.6	8.2	2.5	0.3	3.3
60		$Cu(NO_3)_2$	$NaNO_3$	1[b]	20.6	20.3	0.2	0.1	0.1	3.2
32	$Zr(OH)_x$	$Cu(NO_3)_2$	-		40.1	17.4	21.2	1.3	0.1	17
61		$Cu(NO_3)_2$	H_3BO_3	0.5[c]	52.3	25.1	23.4	3.6	0.2	6.5
62		$Cu(NO_3)_2$	$CuSO_4$	0.1[d]	43.3	19.1	22.2	1.9	0.1	12
63		$Cu(NO_3)_2$	$CuSO_4$	1[d]	38.1	22.4	10.9	4.8	0.1	2.3
64		$Cu(CH_3COO)_2$	-		49.5	23.2	24.2	1.9	0.2	12
65		$CuCl_2$	-		1.6	0.7	0.3	0.2	0.4	1.7
66		$CuSO_4$	-		88.0	1.2	0.0	0.0	86.8[e]	

Catalyst: 200 mg, ethanol: 20%, N_2: balance, total flow rate: 20 mL·min^{-1}, 493 K, 1 atm. Substrate: see Fig. 8.
[a] 10 wt% as Cu, calcination temp. 673 K; [b] as Na; [c] as B; [d] as S; [e] diethyl ether 56.4%, ethene 30.4%; [f] AcOEt/C4-al,ol

yields were not significantly affected compared to C4-al,ol compounds. It shows that acid site on the surface promote acetaldehyde condensation reaction, the site of which is independent of ethyl acetate formation.

In the present study, ethyl acetate formation could be promoted for the supported copper catalyst independently of the support crystalline phase of ZrO_2. During catalytic test copper species on the surface was reduced to be metallic. Then, the interface between metallic Cu and ZrO_2, and surface acid-base property characteristics to ZrO_2 is considered to key issue for ethyl acetate formation, as in other reports [13,46,47]. The amount of metal-support interface should influence on the catalytic performance. Note formed ethyl acetate / C4-al,ol ratio was independent of the apparent Cu density for each crystalline phase, shown in Fig. 14. It suggests that Cu dispersion was not the key issue in controlling the product selectivity. The coexistence of a strong acid site was suggested to promote acetaldehyde condensation to form C4-al,ol, indicating that precise tuning of surface acid-base property including amounts and the maximum strength are important. The contribution of the surface acid-base property of a catalyst to the reaction selectivity discussed here is only based on empirical evidences from activity tests. We have not obtained direct evidence about acid-base property of a catalyst such as TPD experiments and activity test for some index reactions yet. A more detailed investigation about acid-base properties of the catalysts studied including condensation of acetaldehyde itself is needed and will be carried out in the future.

5. Conclusions

The purpose of the present study is to clarify effect of crystalline phase of ZrO_2 for Cu on direct ethyl acetate synthesis from ethanol. Therefore, we prepared 29 kinds of Cu-ZrO_2 catalysts with different crystalline phase (amorphous, monoclinic, tetragonal-type catalyst) from the same Zr source. Catalysts with the same crystal phase were also prepared by several different methods; i.e., calcination temperature, hydrothermal treatment, metal-ion pre doping, and so forth.

The crystalline phase dependency of ZrO_2 phase on direct ethyl acetate synthesis was evaluated by ethyl acetate yields and product ratio; (ethyl acetate yield) / (sum of butenyl/butyl-alcohols/aldehydes yields). Amorphous-type catalyst exhibited the highest selective index, and the order of suitable crystalline phase without any modification was as follows; amorphous-type >> tetragonal-type > monoclinic-type. Monoclinic ZrO_2 itself possesses has active sites that promote the aldehyde condensation effectively; probably strong acid sites; which reduces ethyl acetate selectivity. Amorphous ZrO_2 is suggested to be less active for the condensation, resulting that high selectivity for ethyl acetate synthesis could be done. Acidity poisoning by addition of Na ion to monoclinic-type catalysts increased ethyl acetate selectivity, whereas acidity promotion to amorphous-type catalysts decreased the selectivity.

CRediT authorship contribution statement

Takashi Yamamoto: Conceptualization, Investigation, Writing.

Hirotaka Mine: Investigation. **Shoki Katada:** Investigation. **Taketo Tone**: Validation.

Declaration of Competing Interest

The authors declare that they have no known competing financial interests or personal relationships that could have appeared to influence the work reported in this paper.

Data Availability

No data was used for the research described in the article.

Acknowledgements

TY acknowledges to Daiichi Kigenso Kagaku Kogyo Co., Ltd for providing the standard sample set of ZrO_2 based catalysts. JRC (Japan Reference Catalyst) catalysts were supplied by the Catalyst Society of Japan. This work was partially supported by JSPS KAKENHI Grant Number 19K05150 and 22K05287.

Appendix A. Supporting information

Supplementary data associated with this article can be found in the online version at doi:10.1016/j.apcatb.2023.122433.

References

[1] C. Angelici, B.M. Weckhuysen, P.C.A. Bruijnincx, Chemocatalytic conversion of ethanol into butadiene and other bulk chemicals, ChemSusChem 6 (2013) 1595–1614.
[2] N.M. Eagan, M.D. Kumbhalkar, J.S. Buchanan, J.A. Dumesic, G.W. Huber, Chemistries and processes for the conversion of ethanol into middle-distillate fuels, Nat. Rev. Chem. 3 (2019) 223–249.
[3] J. Sun, Y. Wang, Recent advances in catalytic conversion of ethanol to chemicals, ACS Catal. 4 (2014) 1078–1090.
[4] K. Takeshita, K. Kawamoto, Reduced copper catalyzed conversion of primary alcohols into Esters and ketones, Bull. Chem. Soc. Jpn 51 (1978) 2622–2627.
[5] D.J. Elliott, F. Pennella, The formation of ketones in the presence of carbon monoxide over $CuO/ZnO/Al_2O_3$, J. Catal. 119 (1989) 359–367.
[6] N. Iwasa, N. Takezawa, Reforming of ethanol –dehydrogenation to ethyl acetate and steam reforming to acetic acid over copper-based catalysts–, Bull. Chem. Soc. Jpn 64 (1991) 2619–2623.
[7] K. Inui, T. Kurabayashi, S. Sato, Direct synthesis of ethyl acetate from ethanol carried out under pressure, J. Catal. 212 (2002) 207–215.
[8] K. Inui, T. Kurabayashi, S. Sato, N. Ichikawa, Effective formation of ethyl acetate from ethanol over Cu-Zn-Zr-Al-O catalyst, J. Mol. Catal. A Chem. 216 (2004) 147–156.
[9] L. Wang, W. Zhu, D. Zheng, X. Yu, J. Cui, M. Jia, W. Zhang, Z. Wang, Direct transformation of ethanol to ethyl acetate on Cu/ZrO_2 catalyst, React. Kinet. Mech. Catal. 101 (2010) 365–375.
[10] A.B. Gaspar, F.G. Barbosa, S. Letichevsky, L.G. Appel, The one-pot ethyl acetate syntheses: The role of the support in the oxidative and the dehydrogenative routes, Appl. Catal. A Gen. 380 (2010) 113–117.
[11] E. Santacesaria, G. Carotenuto, R. Tesser, M. Di Serio, Ethanol dehydrogenation to ethyl acetate by using copper and copper chromite catalysts, Chem. Eng. J. 179 (2012) 209–220.
[12] A.G. Sato, D.P. Volanti, I.C. de Freitas, E. Longo, J.M.C. Bueno, Site-selective ethanol conversion over supported copper catalysts, Catal. Commun. 26 (2012) 122–126.
[13] A.G. Sato, D.P. Volanti, D.M. Meira, S. Damyanova, E. Longo, J.M.C. Bueno, Effect of the ZrO_2 phase on the structure and behavior of supported Cu catalysts for ethanol conversion, J. Catal. 307 (2013) 1–17.
[14] M.D. Rhodes, A.T. Bell, The effects of zirconia morphology on methanol synthesis from CO and H_2 over Cu/ZrO_2 catalysts: Part I. Steady-state studies, J. Catal. 233 (2005) 198–209.
[15] M.D. Rhodes, K.A. Pokrovski, A.T. Bell, The effects of zirconia morphology on methanol synthesis from CO and H_2 over Cu/ZrO_2 catalysts: Part II. Transient-response infrared studies, J. Catal. 233 (2005) 210–220.
[16] T. Witoon, J. Chalorngtham, P. Dumrongbunditkul, M. Chareonpanich, J. Limtrakul, CO_2 hydrogenation to methanol over Cu/ZrO_2 catalysts: Effects of zirconia phases, Chem. Eng. J. 293 (2016) 327–336.
[17] S. Tada, S. Kayamori, T. Honma, H. Kamei, A. Nariyuki, K. Kon, T. Toyao, K. Shimizu, S. Satokawa, Design of interfacial sites between Cu and amorphous ZrO_2 dedicated to CO_2-to-methanol hydrogenation, ACS Catal. 8 (2018) 7809–7819.
[18] T. Yamamoto, A. Orita, T. Tanaka, Structural analysis of tungsten-zirconium oxide catalyst by W K-edge and L1-edge XAFS, X-Ray Spectrom. 37 (2008) 226–231.
[19] T. Yamamoto, A. Teramachi, A. Orita, A. Kurimoto, T. Motoi, T. Tanaka, Generation of strong acid sites on yttrium-doped tetragonal ZrO_2-supported tungsten oxides: effects of dopant amounts on acidity, crystalline phase, kinds of tungsten species, and their dispersion, J. Phys. Chem. C. 120 (2016) 19705–19713.
[20] K.T. Jung, A.T. Bell, The effects of synthesis and pretreatment conditions on the bulk structure and surface properties of zirconia, J. Mol. Catal. A Chem. 163 (2000) 27–42.
[21] T. Taguchi, J. Harada, A. Kiku, K. Tohji, K. Shinoda, Development of a new in-laboratory XAFS apparatus based on new concept, J. Synchrotron Radiat. 8 (2001) 363–365.
[22] T. Yamamoto, S. Mori, T. Kawaguchi, T. Tanaka, K. Nakanishi, T. Ohta, J. Kawai, Evidence of a strained pore wall structure in mesoporous silica FSM-16 studied by X-ray absorption spectroscopy, J. Phys. Chem. C 112 (2008) 328–331.
[23] T. Taguchi, T. Ozawa, H. Yashiro, REX2000: Yet another XAFS analysis package, Phys. Scr. T115 (2005) 205–206.
[24] H. Nishizawa, N. Yamasaki, K. Matsuoka, H. Mitsushio, Crystallization and transformation of zirconia under hydrothermal conditions, J. Am. Ceram. Soc. 65 (1982) 343–346.
[25] R.P. Denkewicz Jr., K.S. TenHuisen, J.H. Adair, Hydrothermal crystallization kinetics of m-ZrO_2 and t-ZrO_2, J. Mater. Res. 5 (1990) 2698–2705.
[26] T. Yamamoto, Assignment of pre-edge peaks in K-edge x-ray absorption spectra of 3d transition metal compounds: Electric dipole or quadrupole? X-Ray Spectrom. 37 (2008) 572–584.
[27] N.G. Schmahl, J. Barthel, G.F. Eikerling, Röntgenographische Untersuchungen an den Systemen MgO-CuO und NiO-CuO, Z. Anorg. Allg. Chem. 332 (1964) 230–237.
[28] K. Tanabe, M. Misono, Y. Ono, H. Hattori, New Solid Acids and Bases, Kodansha, Tokyo, 1989.
[29] A. Auroux, P. Artizzu, I. Ferino, R. Monaci, E. Rombi, V. Solinas, G. Petrini, Dehydration of 4-methylpentan-2-ol over lanthanum and cerium oxides, J. Chem. Soc., Faraday Trans. 92 (1996) 2619–2624.
[30] T. Yamamoto, T. Tanaka, T. Matsuyama, T. Funabiki, S. Yoshida, Alumina-supported rare-earth oxides characterized by acid-catalyzed reactions and spectroscopic methods, J. Phys. Chem. B 105 (2001) 1908–1916.
[31] M.G. Cutrufello, I. Ferino, R. Monaci, E. Rombi, V. Solinas, Acid-base properties of zirconium, cerium and lanthanum oxides by calorimetric and catalytic investigation, Top. Catal. 19 (2002) 225–240.
[32] Y. Ono, H. Hattori, Solid Base Catalysis, Tokyo Institute of Technology Press, Berlin, 2011.
[33] H. Hattori, Y. Ono, Solid Acid Catalysis, Pan Stanford, Singapore, 2015.
[34] T. Yamamoto, A. Kurimoto, Ga ion-doped ZrO_2 catalyst characterized By XRD, XAFS, and 2-butanol decomposition, Anal. Sci. 36 (2020) 41–46.
[35] M. Bhagwat, A.V. Ramaswamy, A.K. Tyagi, V. Ramaswamy, Rietveld refinement study of nanocrystalline copper doped zirconia, Mater. Res. Bull. 38 (2003) 1713–1724.
[36] G. Štefanić, S. Musić, M. Ivanda, Effect of Cu^{2+} ion incorporation on the phase development of ZrO_2-type solid solutions during the thermal treatments, J. Alloy. Compd. 491 (2010) 536–544.
[37] R.D. Shannon, Revised effective ionic radii and systematic studies of interatomic distances in halides and chalcogenides, Acta Crystallogr. Sect. A Found. Crystallogr. 32 (1976) 751–767.
[38] S. Tada, K. Oshima, Y. Noda, R. Kikuchi, M. Sohmiya, T. Honma, S. Satokawa, Effects of Cu precursor types on the catalytic activity of Cu/ZrO_2 toward methanol synthesis via CO_2 hydrogenation, Ind. Eng. Chem. Res. 58 (2019) 19434–19445.
[39] W. Ji, Y. Chen, H.H. Kung, Vapor phase aldol condensation of acetaldehyde on metal oxide catalysts, Appl. Catal. A 161 (1997) 93–104.
[40] V.V. Ordomsky, V.L. Sushkevich, I.I. Ivanova, Study of acetaldehyde condensation chemistry over magnesia and zirconia supported on silica, J. Mol. Catal. A Chem. 333 (2010) 85–93.
[41] V.L. Sushkevich, I.I. Ivanova, Mechanistic study of ethanol conversion into butadiene over silver promoted zirconia catalysts, Appl. Catal. B Environ. 215 (2017) 36–49.
[42] K. Pokrovski, K.T. Jung, A.T. Bell, Investigation of CO and CO_2 adsorption on tetragonal and monoclinic zirconia, Langmuir 17 (2001) 4297–4303.
[43] N. Yamamoto, S. Sato, R. Takahashi, K. Inui, Synthesis of 3-buten-1-ol from 1,4-butanediol over ZrO_2 catalyst, J. Mol. Catal. A Chem. 243 (2006) 52–59.
[44] A. Auroux, P. Artizzu, I. Ferino, V. Solinas, G. Leofanti, M. Padovan, G. Messina, R. Mansani, Dehydration of 4-methylpentan-2-ol over zirconia catalysts, J. Chem. Soc. Faraday Trans. 91 (1995) 3263–3267.
[45] K. Tanabe, T. Takeshita, Catalytic activity and acidic property of solid metal sulfates, Adv. Catal. (1967) 315–349.
[46] I. Ro, Y. Liu, M.R. Ball, D.H.K. Jackson, J.P. Chada, C. Sener, T.F. Kuech, R. J. Madon, G.W. Huber, J.A. Dumesic, Role of the Cu-ZrO_2 interfacial sites for conversion of ethanol to ethyl acetate and synthesis of methanol from CO_2 and H_2, ACS Catal. 6 (2016) 7040–7050.
[47] H. Miura, K. Nakahara, T. Kitajima, T. Shishido, Concerted functions of surface acid-base pairs and supported copper catalysts for dehydrogenative synthesis of esters from primary alcohols, ACS Omega 2 (2017) 6167–6173.